Contents lists available at ScienceDirect

Food Research International

journal homepage: www.elsevier.com/locate/foodres

Lactoferrin-based nanoparticles as a vehicle for iron in food applications – Development and release profile

CrossMark

Joana T. Martins [a,*], Susana F. Santos [a], Ana I. Bourbon [a], Ana C. Pinheiro [a,b], África González-Fernández [c], Lorenzo M. Pastrana [d], Miguel A. Cerqueira [d], António A. Vicente [a]

[a] Centre of Biological Engineering, University of Minho, Campus de Gualtar, 4710-057 Braga, Portugal
[b] Instituto de Biologia Experimental e Tecnológica, Avenida da República, Quinta-do-Marquês, Estação Agronómica Nacional, Apartado 12, 2781-901 Oeiras, Portugal
[c] Immunology, Biomedical Research Center (CINBIO) and Institute of Biomedical Research of Vigo (IBIV), University of Vigo, Campus As Lagoas, Marcosende, 36310 Vigo, Pontevedra, Spain
[d] International Iberian Nanotechnology Laboratory, Av. Mestre José Veiga s/n, 4715-330 Braga, Portugal

ARTICLE INFO

ABSTRACT

This study aims at developing and characterizing bovine lactoferrin (bLf) nanoparticles as an iron carrier. bLf nanoparticles were characterized in terms of size, polydispersity index (PdI), electric charge (ζ-potential), morphology, structure and stability over time. Subsequently, iron release experiments were performed at different pH values (2.0 and 7.0) at 37 °C, in order to understand the release mechanism. bLf (0.2%, w/v) nanoparticles were successfully produced by thermal gelation (75 °C for 20 min). bLf nanoparticles with 35 mM $FeCl_3$ showed an iron binding efficiency value of approximately 20%. The nanoparticles were stable (i.e. no significant variation of size and PdI of the nanoparticles) for 76 days at 4 °C and showed to be stable between 4 and 60 °C and pH 2 and 11. Release experiments at pH 2 showed that iron release could be described by the linear superposition model (explained by Fick and relaxation phenomenon). On the contrary, the release mechanism at pH 7 cannot be described by either Fick or polymer relaxation behaviour. In general, results suggested that bLf nanoparticles could be used as an iron delivery system for future food applications.

© 2016 Elsevier Ltd. All rights reserved.

1. Introduction

Iron deficiency affects ca. two billion people worldwide in developing and mainly in developed countries (Martins et al., 2015). The best strategy to overcome this is to include in the diet a wide variety of foods rich in iron (Mason, Lotfi, Dalmiya, Spethuramen, & Deitchler, 2001). However, iron incorporated into complex food systems presents various problems such as oxidation and precipitation (Nicolai, Britten, & Schmitt, 2011; Van der Meer, Bovee-Oudenhoven, Sesink, & Kleibeuker, 1998; Wapnir, 1990). Thus, carrier systems that can actually transport and protect iron efficiently represent a field of great interest in food industry.

Several types of delivery systems at nanoscale have been developed in order to improve effectiveness and biocompatibility of bioactive compounds (Zariwala, Farnaud, Merchant, Somavarapu, & Renshaw, 2014), being nanoparticles one of these examples. These nanoparticles can be developed from natural (e.g. β-lactoglobulin and alginate) or synthetic (e.g. poly(N-isopropylacrylamide)) materials (Cerqueira et al., 2013; Fuciños et al., 2014). Additionally, they present a large surface area that can be used as a functionalization surface to specific targets, which are not accessible to macro- or microscaled particles (Cerqueira

et al., 2014; Fuciños et al., 2014; Martins et al., 2015). In the food industry, the use of nanoparticles composed of proteins constitutes an interesting strategy for encapsulation and protection of micronutrients such as iron (Bourbon et al., 2015; Chen, Remondetto, & Subirade, 2006; Goldberg, Langer, & Xinqiao, 2007).

Gelling proteins, in particularly globular proteins (e.g. egg white, soy and whey proteins), have attracted much attention over the years due to their physico-chemical properties and industrial relevance (Clark, Kavanagh, & Ross-Murphy, 2001; Nicolai & Durand, 2013). Whey proteins (such as β-lactoglobulin and lactoferrin) have been widely used in food products due to their high nutritional value and gelation capacity (Ramos et al., 2014; Xiong & Kinsella, 1990). The bovine lactoferrin (bLf) from milk is a single-chain glycoprotein of the transferrin family with 703 amino acids, folded into two globular lobules, with a molecular weight of about 80 kDa and an isoelectric point (pI) around 8–9 (Levay & Viljoen, 1995). bLf is also of interest due to its biological properties such antibacterial, antiviral, immunomodulatory and high iron binding capacity (Adlerova, Bartoskova, & Faldyna, 2008; Brock, 2002; Levay & Viljoen, 1995). In order to form gels, bLf requires thermal treatment or addition of an agent for protein denaturation. The temperature, pH and ionic strength, for example, affect gel characteristics (Bourbon et al., 2015; Lefèvre & Subirade, 2000; Ziegler & Foegeding, 1990). Thermal gelation of proteins usually requires a heating step to unfold the native protein, followed by an aggregation process to give a three-dimensional

* Corresponding author.
E-mail address: joanamartins@deb.uminho.pt (J.T. Martins).

network (at nano-scale). Gelation of proteins is one of the most used methods for development of protein aggregates and at high concentrations is used to form gels. When low concentrations are used is possible to produce nanoparticles (Bourbon et al., 2015; Ramos et al., 2014). After the heating step where protein denatures and polymerizes, the cooling step and subsequent salt addition are the following events, which induce protein aggregation (Remondetto, Paquin, & Subirade, 2002). Some examples of commonly used salts are calcium chloride ($CaCl_2$), chloride sodium (NaCl), magnesium chloride ($MgCl_2$), magnesium sulfate ($MgSO_4$) and iron (III) chloride ($FeCl_3$) (Bourbon, Cerqueira, & Vicente, 2016; Roff & Foegeding, 1996). In this work, a ferric salt (i.e. $FeCl_3$) was chosen due to Fe^{3+} affinity to bLf which could address iron deficiency (Kanyshkova, Buneva, & Nevinsky, 2001). The gelation of proteins opens up interesting opportunities to produce innovative food-grade carriers for nutritional compounds (Remondetto et al., 2002). Therefore, bLf nanoparticles may be useful in food and pharmaceutical applications, e.g. to modify the optical or rheological properties of products, or to encapsulate and deliver bioactive ingredients. Moreover, understanding the molecules' release mechanisms by using mathematical modeling is essential for the design of nanoparticle-based delivery systems. This will allow foreseeing if the developed systems behaviour is appropriated to food products and consequently, to human consumption.

The main objectives of this study were the development and characterization of bLf-based nanoparticles as iron vehicle for food applications, and to highlight some of the factors that influence their properties. Additionally, iron release mechanisms from bLf nanoparticle at different pH were evaluated.

2. Material and methods

2.1. Materials

Purified bLf powder was obtained from DMV International (USA). This powder contained (expressed as a dry weigh percentage) 96% protein, 0.5% ash, 3.5% moisture and 0.012% iron (data supplied by the manufacturer). Iron chloride (III) ($FeCl_3$) (97% purity) was obtained from Panreac (Barcelona, Spain). Phosphate buffer saline (PBS) and hydrochloric acid (HCl) (36.5–38.0% purity) were purchased from Sigma–Aldrich Chemical Co. Ltd. (St. Louis, MO, USA). Potassium chloride and nitric acid (35% purity) were obtained from Merck (Darmstadt, Germany); sodium hydroxide (NaOH) was obtained from Fisher Scientific (UK). All samples were prepared with deionized water.

2.2. bLf nanoparticles preparation

2.2.1. Protein solution preparation

The nanoparticle preparation was based in the methodology used by other authors with some modifications (Bengoechea, Peinado, & McClements, 2011). Briefly, 0.2% (w/v) of bLf solution was dissolved in distilled water under agitation for 1 h at 25 °C. Then, pH of the solutions was adjusted to 7 using 1 M NaOH and/or 1 M HCl when necessary. According to Bengoechea et al. (2011), protein solutions (0.2% bLf, pH 7) under specific thermal conditions (i.e. 75 °C and holding time of 20 min) are favourable to the formation of nanoparticles. In order to study if the same conditions (i.e. protein concentration, pH, temperature and holding time) were adjusted to our work, these experimental conditions were used for the formation of bLf nanoparticles with $FeCl_3$ salt.

2.2.2. pH treatment

After agitation for 1 h, bLf solution was adjusted to different values of pH (4, 7 and 10) with 0.1 M HCl or NaOH (Riedel-de Haen, Germany). A holding time of 20 min at 75 °C was chosen based on preliminary work (results not shown) and in the optimum values reported (Bengoechea et al., 2011).

2.2.3. Thermal treatment

In order to study the effect of different temperatures in bLf behaviour, bLf protein solutions (0.2% bLf, pH 7) were subjected to different heat treatments: temperature (60–90 °C) and holding times (0–60 min).

2.2.4. Salt concentration

The effect of $FeCl_3$ salt on the protein aggregation in bLf solutions (0.2% bLf, pH 7) was evaluated by changing salt concentration of the solutions between 0 and 55 mM. Solutions were heated at 75 °C for 20 min and then different $FeCl_3$ concentrations were added.

2.3. bLf nanohydrogel characterization

2.3.1. Determination of size, polydispersity index (PdI) and ζ-potential

Size, PdI and ζ-potential of nanoparticles were determined using a dynamic light scattering (DLS) device (Zetasizer Nano ZS, Malvern Instruments, UK). The intensity-weighted size mean distribution (i.e. Z-average diameter) is reported for all size DLS data of the nanoparticles. The measurements were carried out at 25 °C. Each sample was analyzed in a folded capillary cell. Three true replicates were conducted, with three readings for each sample. Results are given as the average ± standard deviation of the experimental values.

2.3.2. Determination of protein solutions turbidity

The turbidity of protein solutions was analyzed using an UV/visible spectrophotometer at 600 nm (Synergy HT, Bio-Tek, Winooski, USA), and deionized water was used as blank sample.

The turbidity was analyzed in samples of protein solution (0.2% bLf, pH 7) that were heated at 60, 70, 75, 80 or 90 °C. From each solution, a sample was removed every 5 min, until the end of heating process (60 min). The measurements were made in triplicate and experimental values are given as the average ± standard deviation.

The turbidity of protein samples (0.2% bLf, pH 7, heating 75 °C for 20 min) with different $FeCl_3$ concentrations (0, 10, 35 and 55 mM) were analyzed. The experiments were performed in triplicate and the results are expressed in average ± standard deviation.

2.3.3. Transmission electron microscopy (TEM) measurement

The morphology of bLf nanoparticles with or without iron was evaluated on a Zeiss EM 902 A (Germany) microscope at a voltage of 80 kV. The samples were placed in carbon coated copper grids and left to dry at room temperature.

2.3.4. Fourier transform infrared (FTIR) spectroscopy

FTIR spectra of bLf powder, bLf powder and $FeCl_3$ mixture, bLf nanoparticles and bLf nanoparticles with $FeCl_3$ samples were determined using a FTIR spectrophotometer (Perkin-Elmer 16 PC spectrometer, Boston, USA). The samples were ground with spectroscopic grade potassium bromide (KBr) powder and then pressed into 1 mm pellets for FTIR measurement. Spectral scanning was taken in the wavelength region between 4000 and 400 cm^{-1} and 16 scans were conducted. Each spectrum was baseline corrected and the transmittance was normalised.

2.3.5. Iron binding efficiency, loading capacity and yield efficiency

The iron binding efficiency and loading capacity to bLf nanoparticles was determined using the method described by other authors (Azevedo, Bourbon, Vicente, & Cerqueira, 2014). Briefly, bLf nanoparticles with iron were separated from free iron by molecular weight using Amicon® Ultra 0.5 mL 10 K filters (Millipore, Billerica, USA). 500 μL of sample were placed on the Amicon® filter and centrifuged at 14,000 rpm for 20 min (allowing free iron to pass through the filter). At last, the filter was centrifuged in an inverted position at 10,000 rpm for 5 min to allow collecting iron-binding bLf nanoparticles. The iron concentration was determined using Atomic Absorption Spectroscopy

(AAS) (Varian SpectrAA – 250 Plus, California, USA) and an iron standard solution (1.000–0.002 g/L) was used in the measurements.

The nanoparticle yield efficiency was determined using the centrifugation technique described previously. Lbf nanoparticles suspensions were centrifuged, and the pellets, formed from bLf nanoparticles were recovered, freeze-dried and then weighed.

The percentage of binding efficiency, loading capacity and yield efficiency were determined using the equations:

$$\%binding = \frac{iron_{total} - iron_{free}}{iron_{total}} \times 100 \qquad (1)$$

$$\%loading\ capacity = \frac{iron_{total} - iron_{free}}{Nps_{total}} \times 100 \qquad (2)$$

$$\%yield\ efficiency = \frac{W_n}{W_t} \times 100 \qquad (3)$$

where $iron_{total}$ represents the total concentration of iron; $iron_{free}$ the concentration of free iron in filtrate; Nps_{total} the total weight of nanoparticles; W_n is the total weight of bLf nanoparticles recovered and W_t is the total weight of bLf used in the formulation.

2.4. Nanoparticles stability under different environmental conditions

Nanoparticles stability was evaluated through the study of the nanoparticles size and PdI under different conditions (i.e. storage time, temperature and pH). The bLf nanoparticles formation was previously optimized - 0.2% bLf prepared at 75 °C for 20 min and with a salt concentration of 35 mM. The turbidity and DLS analysis were used for nanoparticles stability evaluation according to the previous sections (please see Sections 2.3.1. and 2.3.2., respectively).

2.4.1. pH stability
The influence of pH was evaluated by varying the pH of the bLf nanoparticle dispersions between 2 and 12. The pH of the nanoparticle dispersions was adjusted using 1 M NaOH and/or 1 M HCl.

2.4.2. Temperature stability
To assess thermal stability, a bLf nanoparticle dispersions was prepared and analyzed in DLS (i.e. size and PdI) from 4 to 70 °C using 5 °C increment steps with 60 s temperature ramp time.

2.4.3. Storage stability
bLf nanoparticle dispersions were stored at 4 °C in the absence of light and stability studies (i.e. size, PdI and ζ-potential) were conducted over 76 days. Five replicates were performed for each sample.

2.5. In vitro release studies

To determine the iron release from bLf nanoparticles, in vitro release studies were performed at 37 °C under acidic and neutral conditions according to published procedures (Azevedo et al., 2014). These conditions were used foreseeing a potential incorporation of the nanoparticles developed in an acidic or alkaline food matrix and a potential human consumption. Briefly, iron release from bLf nanoparticle was carried out in a dialysis membrane (Biotech CE, Spectrum Laboratories, EUA; MWCO = 3500 Da). Four milliliter of bLf nanoparticle dispersion (approximately 7 mg of collected nanoparticle) was dispersed in dialysis membrane and sealed. The membrane was placed at 37 °C in 50 mL of phosphate buffer solution (PBS) (0.01 M; pH 7.4) or Tris-KCl-HCl buffer solution (0.2 M KCl and 0.2 M HCl; pH 2.0), under magnetic stirring. An aliquot was taken at predetermined time intervals. The total volume of buffer solution was maintained by adding the same volume of fresh buffer solution. The experiments were performed in triplicate.

After in vitro release studies, the total iron ion concentration of each sample was determined using an inductively coupled plasma-optical emission spectrometer (ICP-OES) analysis (Optical Emission Spectrometer OPTIMA 8000 DV, Perkin Elmer). Briefly, 3 mL aliquot was diluted up to 5 mL with 2% nitric acid in order to stabilize samples. The adopted wavelength to determine iron was 238.204 nm and the plasma viewing mode was radial. A calibration curve (1–10 mg/L) was made before the analysis of the samples. Three measurement replicates were conducted. The measurement unit of the total released iron concentration is mg/L.

2.5.1. Release kinetics
Iron release profile from bLf nanoparticle was assessed using a kinetic model that considers both Fickian and Case II transport (linear super-position model - LSM) effects in hydrophilic matrices (Berens & Hopfenberg, 1978):

$$M_t = M_{t,F} + M_{t,R} \qquad (4)$$

where M_t is the total mass released from the polymeric structure, $M_{t,F}$ and $M_{t,R}$ are the contributions of the Fickian and relaxation processes, respectively, at time t.

The Fickian process is described by:

$$M_{t,F} = M_{\infty,F}\left[1 - \frac{6}{\pi^2}\sum_{n=1}^{\infty}\frac{1}{n^2}\,exp(-n^2\,k_F\,t)\right] \qquad (5)$$

where $M_{\infty,F}$ is the compound release at equilibrium, k_F is the Fickian diffusion rate constant. Eq. (5) can be simplified using the first term of Taylor series (Pinheiro, Bourbon, Quintas, Coimbra, & Vicente, 2012):

$$M_{t,F} = M_F\left[1 - \frac{6}{\pi^2}.exp(k_F\,t)\right] \qquad (6)$$

As for polymer relaxation, it is driven by polymer swelling capacity and is then related to the dissipation of stress induced by penetrant entrance and can be described as a distribution of relaxation times, each assuming a first order-type kinetic equation (Berens & Hopfenberg, 1978):

$$M_{t,R} = \sum_i M_{\infty,R_i}\left[1 - exp(-k_{R_i}t)\right] \qquad (7)$$

where, $M_{\infty,Ri}$ are the contributions of the relaxation processes for compound release and k_{Ri} are the relaxation i^{th} rate constants. In order to simplify Eq. (7), it was considered that there was only one main polymer relaxation that influences release, i.e. $i = 1$, as previously stated by Pinheiro et al. (2012).

As a result, LSM for iron release from bLf nanoparticle can be described by:

$$\frac{M_t}{M_\infty} = X\left[1 - \frac{6}{\pi^2}.exp(-k_F t)\right] + (1-X)[1 - exp(-k_R t)] \qquad (8)$$

where X is the fraction of compound released by Fickian process.

This "general" model can then be used to describe pure Fickian, anomalous (i.e. Fickian and polymer relaxation phenomena) or Case II (only polymer relaxation phenomenon) release processes in biopolymeric matrices at nanoscale (Azevedo et al., 2014; Pinheiro et al., 2012). The experimental results were analyzed by fitting Eq. (6) (Fick's second law) and Eq. (8) (LSM) in order to assess the release mechanism involved in iron release from bLf nanoparticle at pH 2 and 7.

2.6. Statistical analysis

SigmaStat 3.1 Software (Systat Software Inc., Chicago, USA) was used for statistical analysis. The comparison of samples was performed by analysis of variance (ANOVA) followed by multiple comparison by

Tukey test ($p < 0.05$). All measurements were performed with three samples and are reported as mean and standard deviations.

Eqs. 6 and 8 were fitted to data by non-linear regression, using STATISTICA™ v7.0 (Statsoft. Inc., USA). The Levenberg-Marquardt algorithm for the least squares function minimization was applied. The adjusted determination coefficient (R^2) and the squared root mean square error (RMSE) (i.e., the square root of the sum of the squared residues (SSE) divided by the regression degrees of freedom) were calculated and residuals inspection for randomness and normality was performed in order to determine regressions quality. Standardised Halved Width (SHW%) (i.e., the ratio between 95% Standard Error and the estimated value) was assessed to determine the precision of the estimated parameters.

3. Results and discussion

3.1. Influence of pH, temperature and salt concentration in the formation of nanoparticles

The formation of protein nanoparticles is influenced by the treatment conditions applied during their production such as: protein concentration, salt source and concentration, pH and temperature. Being so, we can have different behaviours related with chemical characteristics of the protein and salt used. In this work, bLf nanoparticle formation was based on the best conditions (i.e. protein concentration, pH, temperature and holding time) reported by Bengoechea et al. (2011). However, due to different bLf powder composition reported and salt used in that work, the nanoparticle formation was evaluated and confirmed through the individual variation of such parameters (i.e. pH, temperature, holding time and salt concentration).

3.1.1. Effect of pH on nanoparticle formation

The influence of pH on nanoparticles formation was evaluated using protein solutions at different pH (4, 7 and 10) maintaining other parameters constant (i.e. protein concentration, temperature and holding time – 0.2% bLf, 75 °C, 20 min). Fig. 1 shows the size (Fig. 1a), PdI (Fig. 1b) and ζ-potential (Fig. 1c) of the bLf nanoparticles developed when the initial protein solution presents a pH values of 4, 7 and 10.

Nanoparticles formed at pH 7 and 10 showed lower size ranging from 107 to 110 nm, while for pH 4 the size presents a mean value of 383 ± 3 nm (Fig. 1a). Results can be explained by conformational rearrangement of bLf structure and establishment of new intermolecular interactions (e.g. hydrophobic interactions) under acidic conditions which led to extensive bLf aggregation and formation of larger particles (Bengoechea et al., 2011; Sreedhara et al., 2010). At pH 7, nanoparticles have shown to be more stable, having a PdI significantly lower ($p < 0.05$) compared to values obtained at pH 4 and pH 10 (Fig. 1b). Fig. 1c shows that bLf solution changed its charge from positive ζ-potential (28.7 ± 1.0 mV) at pH 4 to negative ζ-potential (-12.9 ± 0.7 mV) at pH 10.0, with a 19.3 ± 0.5 mV ζ-potential value at pH 7. These findings are in agreement with previous studies that reported the same bLf behaviour under different pH values (Bengoechea et al., 2011; Bourbon et al., 2015). Thus, results showed that pH 7 was the most appropriate pH for the formation of bLf nanoparticles.

3.1.2. Effect of heating temperature and holding time on nanoparticle formation

Nanoparticles formation is promoted by bLf denaturation and aggregation (Ramos et al., 2014). It is thus important to study the effect of temperature and holding time in their formation.

In order to evaluate the influence of the heating temperature on bLf nanoparticle formation, temperature was varied between 60 and 90 °C, and size, PdI and ζ-potential of solutions (0.2% bLf, pH 7, 20 min) were determined (Fig. 2).
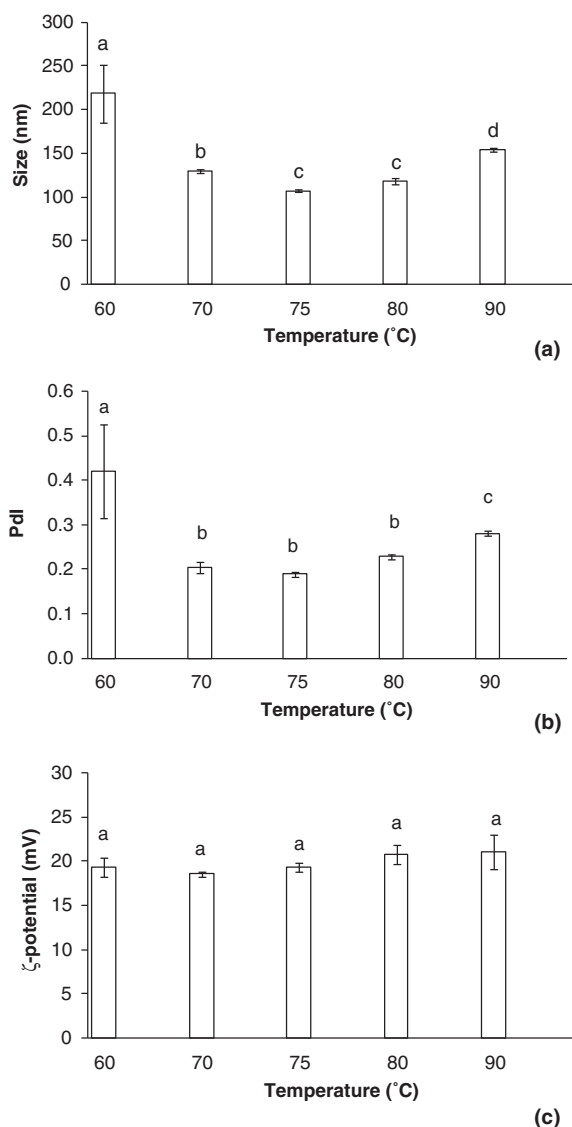
At 75 °C, bLf nanoparticles were formed because sizes were close to 100 nm (Fig. 2a). Between temperatures of 80 and 90 °C there is a
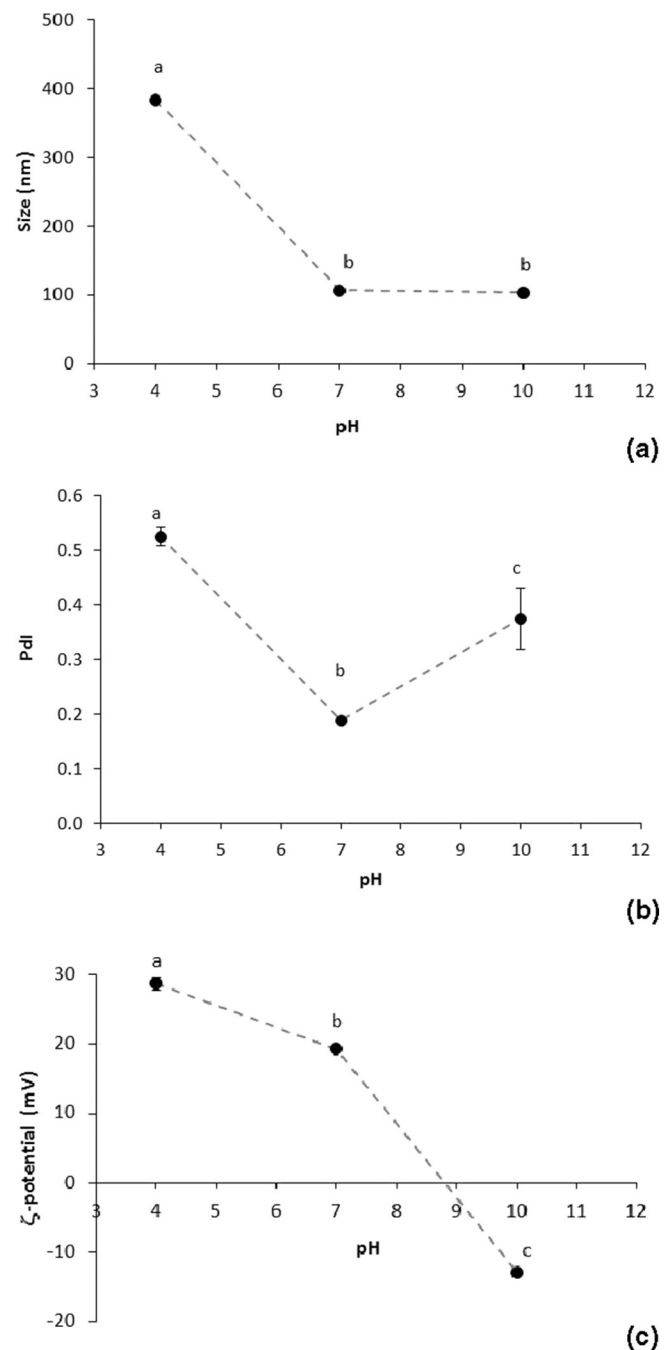
Fig. 1. Effect of pH on the size (a) polydispersity index (PdI) (b) and ζ-potential (c) of the protein solutions (0.2% bLf, 75 °C for 20 min). [a-c] Different letters indicate statistically significant differences between values ($p < 0.05$).

statistically significant increase ($p < 0.05$) in the size and PdI values of the nanoparticles (Fig. 2a and b) which may be explained by the existence of a second thermal denaturation temperature. According to Bengoechea et al. (2011) native Lf has two thermal transitions: the first transition around 60.4 °C corresponding to the apo-lactoferrin form and the second transition around 89.1 °C which corresponds to the holo-lactoferrin form. Brisson, Britten, and Pouliot (2007) also confirmed that heating holo-Lf at 80 °C led to soluble polymer formation whereas apo and native Lf associated into large insoluble aggregates. The thermal aggregation of holo-Lf was mainly driven by non-covalent interactions, with intermolecular thiol/disulfide reactions. The PdI values between 70 and 80 °C showed no statistically significant differences ($p > 0.05$). However, PdI values at 60 °C were higher ($p < 0.05$)
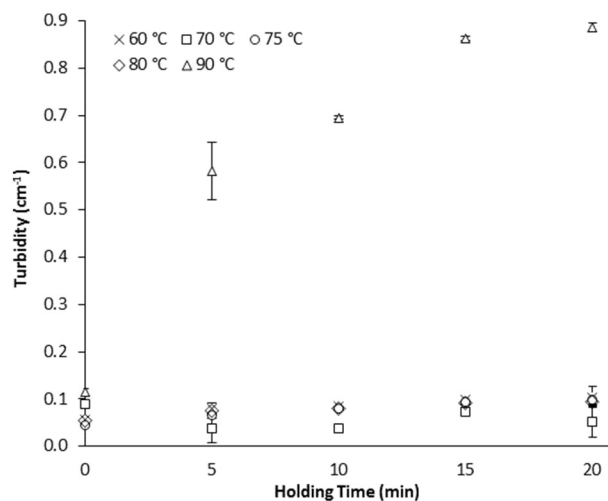
Fig. 2. Effect of temperature on (a) size, (b) PdI and (c) ζ-potential of bLf solutions (0.2% Lf, pH 7). [a-d] Different letters indicate statistically significant differences between values ($p < 0.05$).

Fig. 3. Turbidity (at 600 nm) of bLf protein solutions (0.2% Lf, pH 7) at different temperatures as a function of holding time.

3.1.3. Effect of salt concentration on nanoparticle formation

The effect of increasing $FeCl_3$ concentration (10, 35 and 55 mM) on the nanoparticle formation was evaluated (Table 1). As previously stated, salt has the function of gelling protein after denaturation during heat treatment (Livney, 2010). When the protein is unfolded, the lobes can be in an open conformation, rendering the iron-binding ligands accessible to the iron present in the solution (Abdallah & El Hage Chahine, 2000). Salt addition did not change the size of the nanoparticles (Table 1), however the addition of 55 mM salt increased PdI values ($p < 0.05$) leading to a more heterogeneous solution. This behaviour was confirmed by samples' turbidity (Table 1) of which values presented a high standard deviation suggesting a lower stability of nanoparticles. bLf nanoparticles size did not change significantly ($p > 0.05$) at the salt concentrations studied. This may indicate that the electrostatic repulsion forces between positive-charged nanoparticles were strong enough to avoid the nanoparticles aggregation and precipitation (McClements, 2005). ζ-potential remained positive for the various concentrations of salt tested (Table 1). Therefore, according to our results, 10 or 35 mM salt concentrations could be suitable to produce nanoparticles with a good size average, PdI and ζ-potential. Based on this, a higher salt concentration (35 mM) was used for the development of the nanoparticles, because this concentration will promote a higher iron entrapment in bLf nanoparticles and thus a high release.

In summary, heating 0.2% of bLf solution (pH 7) at 75 °C for 20 min alter significantly the size (from 572.6 ± 316.9 nm to 107.1 ± 1.8 nm) and decreases the PdI (0.54 ± 0.25 to 0.17 ± 0.03) of the nanoparticles. The addition of salt (35 mM $FeCl_3$) has no statistically significant influence ($p > 0.05$), neither in size nor in the PdI of bLf nanoparticles when comparing to 0.2% bLf solutions without salt (Table 1).

3.2. bLf nanoparticle characterization

3.2.1. Nanoparticles stability under different environmental conditions

Nanoparticles were characterized for their stability (i.e. storage, thermal stability and pH stability) in order to understand in what type of food product and in what stage of the food processing could bLf nanoparticles be added. During 76 days, size and PdI of the nanoparticles were evaluated and all parameters remained stable (Fig. 4). The ζ-potential was always positive (approximately +18 mV) (data not shown). The thermal stability of the developed nanoparticles (Fig. 5a) was evaluated between 4 and 70 °C. Between 4 and 60 °C, size values did not changed significantly. However, PdI values increased until 55 °C and then, after 60 °C, nanoparticle PdI decreased ($p < 0.05$). This

than the values observed at 70 and 80 °C (Fig. 2b). This can be explained by the fact that Lf denaturation and aggregation through disulfide cross-linking and hydrophobic interactions occur only at temperatures above 60 °C (Bengoechea et al., 2011). All ζ-potential values (Fig. 2c) were positive (around +20 mV) and no statistically significant differences ($p > 0.05$) were observed between samples, because bLf solution pH is below the pI value of Lf (pI ~8–9) (Brock, 2002; Levay & Viljoen, 1995).

bLf solutions turbidity was measured at various heating temperatures, in order to obtain information about protein aggregation during heating (Fig. 3). The turbidity between 60 and 80 °C remained constant, near to zero, for 20 min. However, between 80 and 90 °C, there was a large increase in turbidity for about 0.9 cm^{-1}. The increase in turbidity can be due to the hydrophobic protein aggregation induced by its thermal denaturation (Bengoechea et al., 2011). The influence of increasing holding time in the aggregation of bLf (0.2% bLf, pH 7) at 75 °C for 60 min, instead of only 20 min, was evaluated by measuring the turbidity of bLf solutions (data not shown). After 20 min (up to 60 min), turbidity was constant, suggesting no alteration in the structure of bLf nanoparticles. Therefore, 20 min was considered the adequate holding time to effectively guarantee the bLf aggregation process.

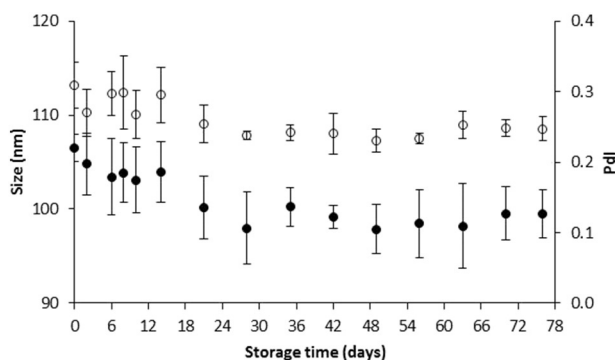| Salt (mM)	Size (nm)	PdI	ζ-potential (mV)	Turbidity (cm^{-1})
0	107.1 ± 1.79 [a]	0.173 ± 0.034 [a]	19.3 ± 0.50 [ac]	0.156 ± 0.029 [a]
10	108.0 ± 0.67 [a]	0.184 ± 0.012 [a]	29.5 ± 2.59 [b]	0.113 ± 0.016 [a]
35	110.0 ± 0.40 [a]	0.218 ± 0.005 [a]	22.1 ± 0.93 [a]	0.109 ± 0.003 [a]
55	106.9 ± 2.19 [a]	0.266 ± 0.023 [b]	17.2 ± 2.21 [c]	0.392 ± 0.386 [a]

Different letters in the same column indicate statistically significant differences between values ($p < 0.05$).

observation may be explained by a first thermal denaturation of bLf around 60 °C as reported by Bengoechea et al. (2011). The stability of the nanoparticles at different pH values was evaluated (Fig. 5b) between pH 2 and 12. Between pH 2 and 11, both size and PdI values were very stable. The good stability of the nanoparticles may be due to the formation of strong covalent or hydrophobic bonds between the molecules of bLf after denaturation (Bengoechea et al., 2011; Steijns & van Hooijdonk, 2000). At pH 12, there was a significant increase ($p < 0.05$) of nanoparticles size which may be due to the low electrostatic repulsion at this pH (Clark, Judge, Richards, Stubbs, & Suggett, 1981; Stading, Langton, & Hermansson, 1993).

3.2.2. bLf nanoparticles morphology, iron binding efficiency, loading capacity and yield efficiency

TEM images (Fig. 6) confirmed bLf nanoparticles formation at the conditions studied (pH 7, 75 °C, 20 min, 35 mM FeCl$_3$) and the size values obtained by DLS (approximately 100 nm). After 1 day (Fig. 6a and b) or 11 days (Fig. 6c and d) of the formation of bLf nanoparticles, the size values remained similar (results also confirmed by DLS) proving the stability of these bLf nanoparticles. Also, Fig. 6 showed that iron (black dots) is present in nanoparticles suggesting binding of iron to bLf nanoparticles.

Nanoparticles exhibited a yield efficiency of 53.8 ± 12.6%, which is in accordance with findings reported by Bagheri, Madadlou, Yarmand, and Mousavi (2014). These authors observed yield efficiency around 54.5% for particles composed by peptides obtained through hydrolysis of whey proteins and then cross-linked by transglutaminase. The iron bound to nanoparticles was quantified by AAS. Approximately, 20% of the iron added to nanoparticles was bound. Depending on the material used to produce the carrier matrix (e.g. β-lactoglobulin, gelatin), there is a great variation in iron binding efficiency (4–90%) in other published works (Cui et al., 2007; De Temmerman, Demeester, De Vos, & De Smedt, 2011; Ofokansi, Winter, Fricker, & Coester, 2010; Remondetto, Beyssac, & Subirade, 2004). The loading capacity of bLf nanoparticles was 2.6 ± 0.7%. This value was in range of other studies using protein-based nanoparticles as bioactive compound carriers. Patel, Hu, Tiwari, and Velikov (2010) obtained loading capacity ranging between 1.5 and 4% for zein-based nanoparticles loaded with curcumin; Yi, Lam, Yokoyama, Cheng, and Zhong (2014) developed β-carotene-loaded β-lactoglobulin nanoparticles with loading capacity of 1.07%; and Yi, Lam, Yokoyama, Cheng, and Zhong (2015) reported loading capacity of β-carotene in sodium caseinate, whey protein isolate, and soybean nanoparticles of 1.07%, 1.05%, and 1.06%, respectively.

3.2.3. Fourier transform infrared (FTIR) spectroscopy analysis

FTIR analyses were used to evaluate the interaction between bLf nanoparticles and iron. Fig. 7 shows FTIR spectra of four different samples (bLf powder, bLf powder and FeCl$_3$ mixture, bLf nanoparticle and bLf nanoparticle with FeCl$_3$). bLf powder showed the characteristic protein absorption band peaks: amide I at 1651 cm^{-1} due to C=O stretching vibration of the peptide group and amide II at 1541 cm^{-1} due to N—H bending with contribution of C—N stretching vibrations (Barth, 2007). The strong band at 3310 cm^{-1} represented O—H stretching, indicating that residual water was present in the sample. In the range 2850–3000 cm^{-1}, numerous bands were noted and attributed to C—H stretching vibration, corresponding to the symmetrical and asymmetrical stretching in the –CH$_2$ and –CH$_3$ groups (Delor, Lacoste, Lemaire, Barrois-Oudin, & Cardine, 1996; Haris & Severcan, 1999; Larkin, 2011; Mattos, Viganó, Dutra, Diniz, & Iha, 2002). The broad structure from 900 to 1200 cm^{-1} is due to C—O, C—C stretches and

a)

b)
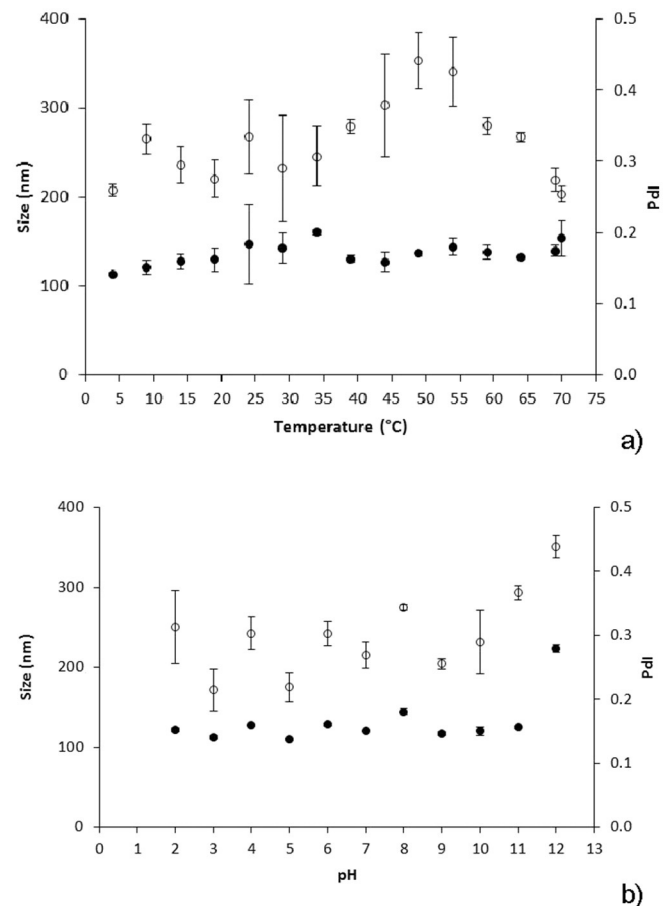
Fig. 5. Effect of a) temperature and b) pH on the size (●) and PdI (○) of bLf nanoparticles with 35 mM FeCl$_3$.

**Fig. 4.** Effect of storage time at 4 °C on the size (●) and PdI (○) of bLf nanoparticles with 35 mM of FeCl$_3$.
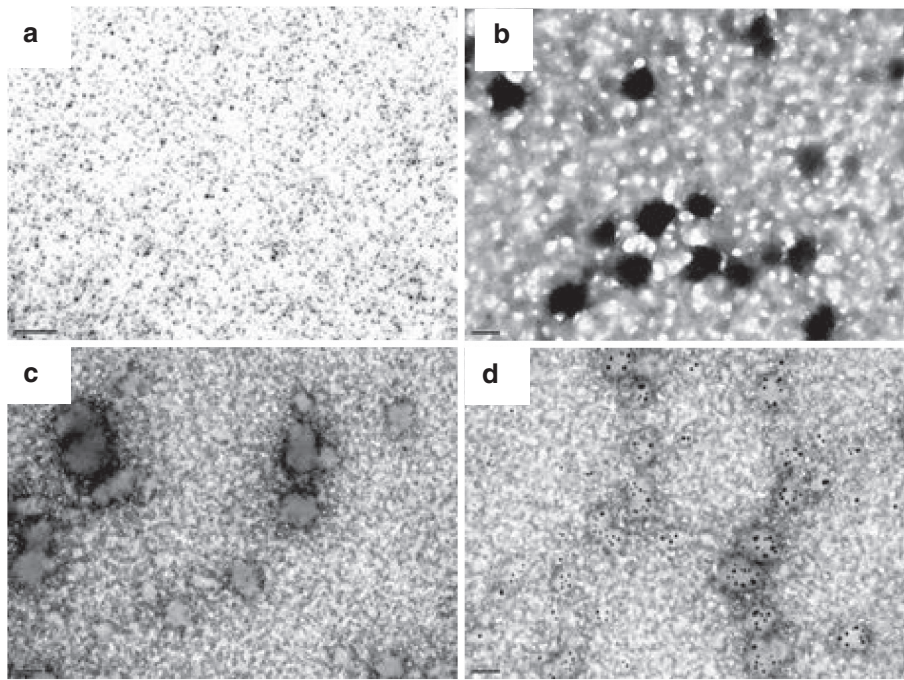
Fig. 6. Transmission electron micrographs (TEM) of 0.2% bovine lactoferrin nanoparticles prepared at pH 7, 75 °C, 20 min and 35 mM FeCl₃ during storage at (a) day 1 (5 μm scale bar); (b) day 1 (100 nm scale bar); (c) day 11 (200 nm scale bar); and (d) day 11 (100 nm scale bar).

C—O—H, C—O—C deformation of bLf (Barth, 2007). The band appearing around 700–600 cm^{-1} can be assigned to —NH₂ and —NH wagging (Xavier, Chaudhari, Verma, Pal, & Pradeep, 2010).

By comparing bLf powder and bLf nanoparticles spectra, it can be seen that after the formation of the nanoparticle there is a decrease of the intensity in the 400–4000 cm^{-1} region. However, typical bands from bLf powder (e.g. amide I and amide II bands) did not change their position, thus confirming that only minor changes occurred in the bLf. The same behaviour (i.e reduced peak intensity) was observed for bLf and FeCl₃ powder mixture (without heat treatment). A weakening of peak intensities in the amide I and amide II regions (around 1650

and 1541 cm^{-1}, respectively) was observed, which could be explained by a molecular interaction between bLf and FeCl₃. However, a more marked change in FTIR pattern of bLf nanoparticle was observed when FeCl₃ was added suggesting that the thermal treatment potentiated the interaction between the bLf and iron. bLf nanoparticle peak intensity at ~1541 cm^{-1} (amide II) decreased. The presence of FeCl₃ in bLf nanoparticle also results in an increase of the amide I peak intensity and in a shift in this region from ~1650 cm^{-1} to 1623 cm^{-1}. Thus, intensity reduction around amide II (N—H deformation) peak and amide I (primarily C═O stretching vibration) peak shift point to altered bond energies and potential molecular interaction between Fe-bLf. Also, a frequency
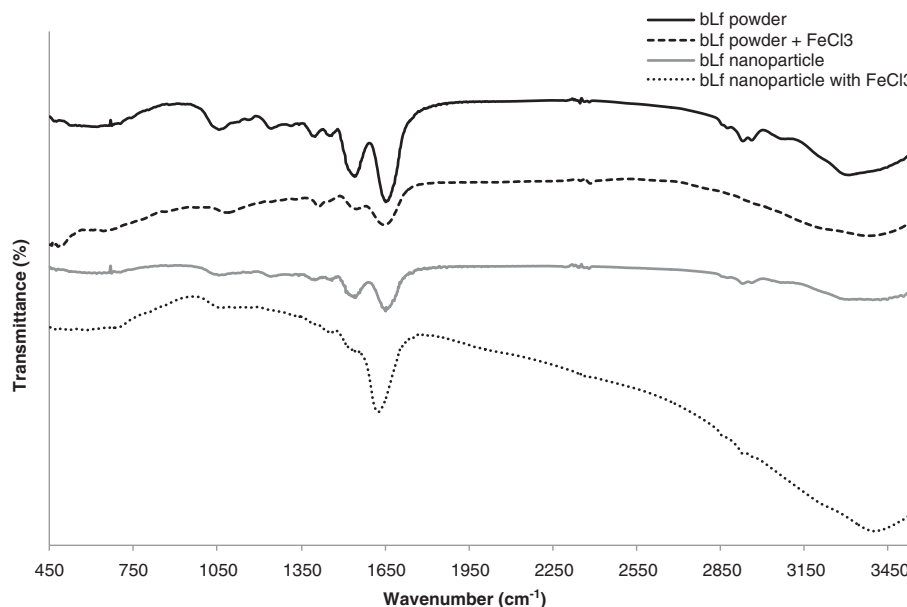
Fig. 7. FTIR spectrum of bLf powder, bLf powder and FeCl₃ mixture, bLf nanoparticles and bLf nanoparticles with FeCl₃ samples in the spectral region between 400 and 4000 cm^{-1}.

shift of the amide I vibration is predominantly the result of a change in C=O and C—N groups of protein subunits (hydrophilic interaction) (Haris & Severcan, 1999; Hoppe, Hulthén, & Hallberg, 2005). Iron has specific site-binding to bLf, which has an impact on the aggregation and gel formation of bLf molecules. When iron is added to the bLf inter-molecular interaction may occur between the former. The binding of iron to bLf caused conformational changes and the molecule became more compact. Iron entered into the open interdomain cleft in each lobe (N- and C-lobe) of bLf, and then the domains closed over the iron atoms (Bokkhim, Bansal, GrØndahl, & Bhandari, 2013).

3.3. In vitro iron release profiles

The experimental release conditions used allowed predicting the iron nanocarriers' behaviour during food production and/or food consumption. To achieve a good carrier formulation, the bLf nanoparticles must protect iron from environmental parameters (e.g. pH, temperature) and prevent the compound from earlier release. Fig. 8 shows the release profile of iron from bLf nanoparticle at pH 2 and 37 °C. Results indicated that the change of the pH of the release medium could lead to different release profiles. This change can be related to structural and charge modifications in the polymer network of bLf nanoparticles (Baker & Baker, 2004).

In order to evaluate the mechanism of iron release from nanoparticles at pH 2 and 7, the experimental results were analyzed by fitting Fick's second law (Eq. (6)) and LSM (Eq. (8)). At pH 7, iron was not released, thus it cannot be described by either Fick or polymer relaxation behaviour (data not shown). The binding of iron to bLf binding site takes place at pH values around 7. A similar behaviour was observed by Martin and de Jong (2012) during iron release from whey protein isolate (WPI) particles. These authors observed a low release of iron at pH 6.5 indicating a good capacity of WPI to keep iron bound, and an increase of iron release at pH 2. Table 2 and Fig. 8 present the regression analysis results of LSM fitting, showing that this model adequately describes experimental data at pH 2 with relatively good regression quality ($R^2 > 0.90$), and almost all parameters were estimated with good precision. On the other hand, iron release mechanism cannot be described only by Fick's behaviour ($R^2 = 0.742$) as can be seen in Fig. 8. Fick's diffusion contribution to the total release of iron from the nanoparticles can be evaluated by X estimation (defined as $M_{\infty,F}/M_t$). It can be observed that for pH 2, $X < 0.5$, which means that Case II transport (polymer relaxation) is the major release mechanism of iron. This suggests that the LSM model can be used to describe the physical mechanism involved in iron release from bLf nanoparticles. Once bLf nanoparticles are a hydrophilic and swellable system, the iron released would result from a combination of diffusion and macromolecular swelling processes. Results are in agreement with Bourbon, Cerqueira,
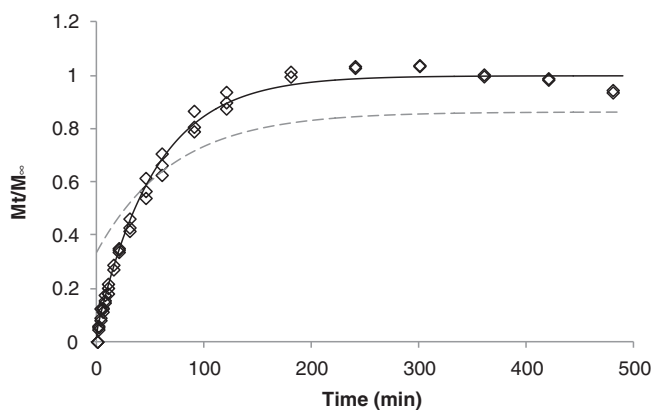
Table 2
Results of Linear Superposition Model (LSM) ($i = 1$) fitting to experimental data of iron release at pH 2 and 37 °C. Quality of the regression based on RMSE and R^2 evaluation. Estimates' precision is evaluated using the SHW% (in parenthesis).

R^2	X	k_F (min^{-1})	k_R (min^{-1})	RMSE
0.990	3.873×10^{-2} (50.28%)	2.068 (607%)	1.845×10^{-2} (9.40%)	4.50×10^{-3}

et al. (2016). These authors found that the release mechanism of bioactive compounds from bLf-glycomacropeptide (bLf-GMP) nanohydrogels at pH 2 and 37 °C can only be described by Fick's diffusion and Case II transport, and relaxation is the governing phenomenon for bioactive compounds release ($X < 0.5$). The relaxation rate constant (k_R) is lower than the Fickian rate constant (k_F) for pH 2. This observation does not mean that Fick's diffusion was higher than polymer relaxation under this condition, but it shows that iron is released more rapidly by Fick's diffusion than by polymer relaxation. Moreover, bLf possesses a lower iron-binding affinity at acidic conditions in accordance to a previous study (Baker & Baker, 2004). Release results may be explained by the interactions between iron and bLf at different pH values. In general, pH modulates protein stability by changing the charges on ionizable groups in the proteins through protonation or deprotonation. Lowering the pH could lead to iron release from bLf nanoparticle due to the destabilisation of the bLf. The loss of non-protein CO_3^{2-} ligand from the iron binding site followed by its protonation is responsible for the destabilisation of the iron site and release of iron at low pH (Bokkhim et al., 2013). It seems that when iron is bound to the bLf molecule, a more closed conformation is adopted. bLf has a relatively high pI (8–9) and therefore tends to be cationic at neutral pH.

4. Conclusions

bLf nanoparticles with iron biding efficiency can be produced under specific conditions. The most effective conditions were the following: 0.2% bLf, pH 7, heating 75 °C for 20 min and adding 35 mM FeCl$_3$. The developed nanoparticles exhibited high thermal, storage time and pH stability. The factor "stability" is very important for the food industry, as it determines the range of foods in that these nanoparticles could be added. The results showed that bLf nanoparticles were stable during 76 days and maintained their characteristics at 4–60 °C and pH 2–11. Additionally, the results of iron release from the nanoparticles allowed the interpretation of the phenomena involved in mass release. This work presents promising results for the use of bLf nanoparticles as vector for iron delivery and food fortification in food industry.

Fig. 8. Release profile of iron from bLf nanoparticle at pH 2, 37 °C. Experimental data (◇); description of Fick's model ($i = 0$) (– – –) and of Linear Superposition Model ($i = 1$) (—).

References

Abdallah, F. B., & El Hage Chahine, J. M. (2000). Transferrins: Iron release from lactoferrin. *Journal of Molecular Biology, 303*, 255–266.
Adlerova, L., Bartoskova, A., & Faldyna, M. (2008). Lactoferrin: A review. *Veterinární Medicína, 53*(9), 457–468.

Azevedo, M. A., Bourbon, A. I., Vicente, A. A., & Cerqueira, M. A. (2014). Alginate/chitosan nanoparticles for encapsulation and controlled release of vitamin B2. *International Journal of Biological Macromolecules*, *71*, 141–146. http://dx.doi.org/10.1016/j.ijbiomac.2014.05.036.

Bagheri, L., Madadlou, A., Yarmand, M., & Mousavi, M. E. (2014). Potentially bioactive and caffeine-loaded peptidic sub-micron and nanoscalar particles. *Journal of Functional Foods*, *6*, 462–469.

Baker, H. M., & Baker, E. N. (2004). Lactoferrin and iron: Structural and dynamic aspects of binding and release. *BioMetals*, *17*, 209–216.

Barth, A. (2007). Infrared spectroscopy of proteins. *Biochimica et Biophysica Acta (BBA) - Bioenergetics*, *1767*(9), 1073–1101. http://dx.doi.org/10.1016/j.bbabio.2007.06.004.

Bengoechea, C., Peinado, I., & McClements, D. J. (2011). Formation of protein nanoparticles by controlled heat treatment of lactoferrin: Factors affecting particle characteristics. *Food Hydrocolloids*, *25*(5), 1354–1360. http://dx.doi.org/10.1016/j.foodhyd.2010.12.014.

Berens, A. R., & Hopfenberg, H. B. (1978). Diffusion and relaxation in glassy polymer powders: 2. Separation of diffusion and relaxation parameters. *Polymer*, *19*(5), 489–496.

Bokkhim, H., Bansal, N., GrØndahl, L., & Bhandari, B. (2013). Physico-chemical properties of different forms of bovine lactoferrin. *Food Chemistry*, *141*(3), 3007–3013. http://dx.doi.org/10.1016/j.foodchem.2013.05.139.

Bourbon, A. I., Cerqueira, M. A., & Vicente, A. A. (2016). Encapsulation and controlled release of bioactive compounds in lactoferrin-glycomacropeptide nanohydrogels: Curcumin and caffeine as model compounds. *Journal of Food Engineering*, *180*, 110–119. http://dx.doi.org/10.1016/j.jfoodeng.2016.02.016.

Bourbon, A. I., Pinheiro, A. C., Carneiro-da-Cunha, M. G., Pereira, R. N., Cerqueira, M. A., & Vicente, A. A. (2015). Development and characterization of lactoferrin-GMP nanohydrogels: Evaluation of pH, ionic strength and temperature effect. *Food Hydrocolloids*, *48*, 292–300. http://dx.doi.org/10.1016/j.foodhyd.2015.02.026.

Brisson, G., Britten, M., & Pouliot, Y. (2007). Heat-induced aggregation of bovine lactoferrin at neutral pH: Effect of iron saturation. *International Dairy Journal*, *17*(6), 617–624. http://dx.doi.org/10.1016/j.idairyj.2006.09.002.

Brock, J. H. (2002). The physiology of lactoferrin. *Biochemistry and Cell Biology*, *80*(1), 1–6. http://dx.doi.org/10.1139/o01-212.

Cerqueira, M. A., Pinheiro, A. C., Silva, H. D., Ramos, P. E., Azevedo, M. A., Flores-López, M. L., ... Vicente, A. A. (2014). Design of bio-nanosystems for oral delivery of functional compounds. *Food Engineering Reviews*, *6*(1–2), 1–19. http://dx.doi.org/10.1007/s12393-013-9074-3.

Chen, L., Remondetto, G. E., & Subirade, M. (2006). Food protein-based materials as nutraceutical delivery systems. *Trends in Food Science & Technology*, *17*(5), 272–283. http://dx.doi.org/10.1016/j.tifs.2005.12.011.

Clark, A., Judge, F., Richards, J., Stubbs, J., & Suggett, A. (1981). Electron microscopy of network structures in thermally-induced globular protein gels. *International Journal of Peptide Research*, *17*, 380–392.

Clark, A. H., Kavanagh, G. M., & Ross-Murphy, S. B. (2001). Globular protein gelation - theory and experiment. *Food Hydrocolloids*, *15*, 383–400.

Cui, F., He, C., Yin, L., Qian, F., He, M., Tang, C., & Yin, C. (2007). Nanoparticles incorporated in Bilaminated films: A smart drug delivery system for oral formulations. *Biomacromolecules*, *8*, 2845–2850.

De Temmerman, M. -L., Demeester, J., De Vos, F., & De Smedt, S. C. (2011). Encapsulation performance of layer-by-layer microcapsules for proteins. *Biomacromolecules*, *12*(4), 1283–1289. http://dx.doi.org/10.1021/bm101559w.

Delor, F., Lacoste, J., Lemaire, J., Barrois-Oudin, N., & Cardine, C. (1996). Photo- and thermal ageing of polychloroprene: Effect of carbon black and crosslinking. *Polymer Degradation and Stability*, *53*, 361–369.

Fuciños, C., Fuciños, P., Míguez, M., Katime, I., Pastrana, L. M., & Rúa, M. L. (2014). Temperature- and pH-sensitive nanohydrogels of poly(N-isopropylacrylamide) for food packaging applications: Modelling the swelling-collapse behaviour. *PloS One*, *9*(2), 1–15. http://dx.doi.org/10.1371/journal.pone.0087190.t001.

Goldberg, M., Langer, R., & Xinqiao, J. (2007). Nanostructured materials for applications in drug delivery and tissue engineering. *Journal of Biomaterials Science, Polymer Edition*, *18*(3), 241–268.

Haris, P. I., & Severcan, F. (1999). FTIR spectroscopic characterization of protein structure in aqueous and non-aqueous media. *Journal of Molecular Catalysis B: Enzymatic*, *7*, 207–221.

Hoppe, M., Hulthén, L., & Hallberg, L. (2005). The relative bioavailability in humans of elemental iron powders for use in food fortification. *European Journal of Nutrition*, *45*(1), 37–44. http://dx.doi.org/10.1007/s00394-005-0560-0.

Kanyshkova, T. G., Buneva, V. N., & Nevinsky, G. A. (2001). Lactoferrin and its biological functions. *Biokhimiya*, *66*(1), 5–13.

Larkin, P. (2011). *Infrared and raman spectroscopy: Principles and spectral interpretation.* San Diego: Elsevier.

Lefèvre, T., & Subirade, M. (2000). Molecular differences in the formation and structure of fine-stranded and particulate β-lactoglobulin gels. *Biopolymers*, *54*, 578–586.

Levay, P. F., & Viljoen, M. (1995). Lactoferrin: A general review. *Haematologica*, *80*, 252–267.

Livney, Y. D. (2010). Milk proteins as vehicles for bioactives. *Current Opinion in Colloid & Interface Science*, *15*(1–2), 73–83. http://dx.doi.org/10.1016/j.cocis.2009.11.002.

Martin, A. H., & de Jong, G. A. H. (2012). Impact of protein pre-treatment conditions on the iron encapsulation efficiency of whey protein cold-set gel particles. *European Food Research and Technology*, *234*(6), 995–1003. http://dx.doi.org/10.1007/s00217-012-1717-8.

Martins, J. T., Ramos, Ó. L., Pinheiro, A. C., Bourbon, A. I., Silva, H. D., Rivera, M. C., ... Vicente, A. A. (2015). Edible bio-based nanostructures: Delivery, absorption and potential toxicity. *Food Engineering Reviews*, *7*(4), 491–513. http://dx.doi.org/10.1007/s12393-015-9116-0.

Mason, J., Lotfi, M., Dalmiya, N., Sethuramen, K., & Deitchler, M. (2001). *The micronutrient report: Current progress and trends in the control of Vitamin A, Iodine, and Iron Deficiences.* Otawa: The Micronutrient Initiative.

Mattos, E., Viganó, I., Dutra, R., Diniz, M., & Iha, K. (2002). Application of FTIR methodologies of transmission and photoacoustic to the characterization of highly energetic materials – Part II. *Quimica Nova*, *25*(5), 722–728.

McClements, D. J. (2005). *Food emulsifications: Principals, practice and tecnhiques* (2nd ed). Boca Raton: CRC Press.

Nicolai, T., & Durand, D. (2013). Controlled food protein aggregation for new functionality. *Current Opinion in Colloid & Interface Science*, *18*(4), 249–256. http://dx.doi.org/10.1016/j.cocis.2013.03.001.

Nicolai, T., Britten, M., & Schmitt, C. (2011). β-Lactoglobulin and WPI aggregates: Formation, structure and applications. *Food Hydrocolloids*, *25*(8), 1945–1962. http://dx.doi.org/10.1016/j.foodhyd.2011.02.006.

Ofokansi, K., Winter, G., Fricker, G., & Coester, C. (2010). Matrix-loaded biodegradable gelatin nanoparticles as new approach to improve drug loading and delivery. *European Journal of Pharmaceutics and Biopharmaceutics*, *76*(1), 1–9. http://dx.doi.org/10.1016/j.ejpb.2010.04.008.

Patel, A., Hu, Y., Tiwari, J. K., & Velikov, K. P. (2010). Synthesis and characterisation of zein–curcumin colloidal particles. *Soft Matter*, *6*(24), 6192–6199.

Pinheiro, A. C., Bourbon, A. I., Quintas, M. A. C., Coimbra, M. A., & Vicente, A. A. (2012). K-carrageenan/chitosan nanolayered coating for controlled release of a model bioactive compound. *Innovative Food Science & Emerging Technologies*, *16*, 227–232. http://dx.doi.org/10.1016/j.ifset.2012.06.004.

Ramos, O. L., Pereira, R. N., Rodrigues, R., Teixeira, J. A., Vicente, A. A., & Xavier Malcata, F. (2014). Physical effects upon whey protein aggregation for nano-coating production. *Food Research International*, *66*, 344–355. http://dx.doi.org/10.1016/j.foodres.2014.09.036.

Remondetto, G. E., Beyssac, E., & Subirade, M. (2004). Iron availability from whey protein hydrogels: An in vitro study. *Journal of Agricultural and Food Chemistry*, *52*, 8137–8143.

Remondetto, G. E., Paquin, P., & Subirade, M. (2002). Cold gelation of β-lactoglobulin in the presence of iron. *Journal of Food Science*, *67*(2), 586–595.

Roff, C. F., & Foegeding, E. A. (1996). Dicationic-induced gelation of pre-denatured whey protein isolate. *Food Hydrocolloids*, *10*(2), 193–198.

Sreedhara, A., Flengsrud, R., Prakash, V., Krowarsch, D., Langsrud, T., Kaul, P., ... Vegarud, G. E. (2010). A comparison of effects of pH on the thermal stability and conformation of caprine and bovine lactoferrin. *International Dairy Journal*, *20*(7), 487–494. http://dx.doi.org/10.1016/j.idairyj.2010.02.003.

Stading, M., Langton, M., & Hermansson, A. -M. (1993). Microstructure and rheological behaviour of particulate β-lactoglobulin gels. *Food Hydrocolloids*, *7*(3), 195–212.

Steijns, J. M., & van Hooijdonk, A. C. M. (2000). Occurrence, structure, biochemical properties and technological characteristics of lactoferrin. *British Journal of Nutrition*, *84*, S11–S17.

Van der Meer, R., Bovee-Oudenhoven, I. M. J., Sesink, A. L. A., & Kleibeuker, J. H. (1998). Milk products and intestinal health. *International Dairy Journal*, *8*(163–170).

Wapnir, R. (1990). *Nutritional factors, proteins, and the absorption of iron and cobalt.* New York: CRC Press.

Xavier, P. L., Chaudhari, K., Verma, P. K., Pal, S. K., & Pradeep, T. (2010). Luminescent quantum clusters of gold in transferrin family protein, lactoferrin exhibiting FRET. *Nanoscale*, *2*(12), 2769. http://dx.doi.org/10.1039/c0nr00377h.

Xiong, Y. L., & Kinsella, J. E. (1990). Mechanism of urea-induced whey protein gelation. *Journal of Agricultural and Food Chemistry*, *38*(10), 1887–1891.

Yi, J., Lam, T. I., Yokoyama, W., Cheng, L. W., & Zhong, F. (2014). Controlled release of β-carotene in β-lactoglobulin–dextran-conjugated nanoparticles' in vitro digestion and transport with Caco-2 monolayers. *Journal of Agricultural and Food Chemistry*, *62*(35), 8900–8907.

Yi, J., Lam, T. I., Yokoyama, W., Cheng, L. W., & Zhong, F. (2015). Beta-carotene encapsulated in food protein nanoparticles reduces peroxyl radical oxidation in Caco-2 cells. *Food Hydrocolloids*, *43*, 31–40.

Zariwala, M. G., Farnaud, S., Merchant, Z., Somavarapu, S., & Renshaw, D. (2014). Ascorbyl palmitate/DSPE-PEG nanocarriers for oral iron delivery: Preparation, characterisation and in vitro evaluation. *Colloids and Surfaces B: Biointerfaces*, *115*, 86–92. http://dx.doi.org/10.1016/j.colsurfb.2013.11.028.

Ziegler, G. R., & Foegeding, E. A. (1990). *The gelation of proteins34.* (pp. 203–298), 203–298. http://dx.doi.org/10.1016/s1043-4526(08)60008-x.